The Nature of Radio-Intermediate Quasars: What is Radio-Loud and what is Radio-Quiet?

Heino Falcke

Astronomy Department, University of Maryland, College Park, MD 20742-2421 (hfalcke@astro.umd.edu)

William Sherwood (p166she@mpifr-bonn.mpg.de)

and

Alok R. Patnaik (apatnaik@mpifr-bonn.mpg.de)

Max-Planck-Institut für Radioastronomie, Auf dem Hügel 69, D-53121 Bonn, Germany

ABSTRACT

We have performed quasi-simultaneous radio flux density measurements at 2.7 and 10 GHz for all PG quasars with radio flux densities between 4-200 mJy. We find that a large fraction of these sources are variable, flat-spectrum quasars. This brings the total fraction of flat-spectrum quasars with a ratio between radio and optical flux of $R > 10$ — a value previously used to define a radio-loud quasar — to 40% in the PG quasar sample. We also find that the median R-parameter of these flat-spectrum quasars is *lower* than those of steep-spectrum radio-loud quasars. This contradicts the predictions of the unified scheme and the idea that all flat-spectrum, core-dominated quasars are relativistically boosted lobe-dominated quasars. We show that this discrepancy is due to a population of flat-spectrum radio-intermediate quasars with $25 < R < 250$ which can neither be explained as relativistically boosted radio-loud quasars nor as normal radio-weak quasars. We point out that a natural explanation for the flat-spectrum radio-intermediate quasars is relativistic boosting in *radio-weak* quasars. If the flat-spectrum radio-intermediate quasars are considered the boosted counterparts to usual radio-weak quasars, their fraction among radio-weak quasars is roughly 10%, similar to the fraction of boosted radio-loud quasars. This would point towards average Lorentz factors of $\gamma_{\rm jet} = 2 - 4$ for radio-loud and radio-weak quasars. The presence of the flat-spectrum radio-intermediate quasars changes the definition of 'radio-loud' and can bias some conclusions drawn from optically selected quasar samples, where $R \simeq 1 - 10$ is used as the dividing line for both, flat- and steep-spectrum quasars. Instead one should use separate R-parameters for the dividing line in steep- ($R \simeq 25$) and flat-spectrum ($R \sim 250$) quasars.

Subject headings: galaxies: active — galaxies: jets — galaxies: nuclei — galaxies: quasars — radio continuum: galaxies

1. Introduction

Since the discovery of quasars[1] it was known that some of them have strong radio emission and others do not. Strittmatter et al. (1980) showed that, in fact, there is a dichotomy in the distribution of the radio emission of quasars, and the studies of radio morphology of quasars have made clear why this is so (Miller, Rawlings, & Saunders 1993; Kellermann et al. 1994, hereinafter K94); while radio-weak quasars show at best diffuse extended emission, most radio-loud quasars are either point-like or have a double-lobed radio structure, very similar to those in Fanaroff-Riley type II (FR-II) radio galaxies. The total flux density at the canonical radio frequency of 5 GHz of the latter is dominated by the steep-spectrum synchrotron emission from the extended radio lobes. Those lobes and a compact radio core in the center of radio-loud quasars are signs of a relativistic radio jet produced by the central engine of the quasar.

This relativistic jet is also one of the keys to the unified scheme for radio galaxies and quasars (e.g. Barthel 1989, see also Urry & Padovani 1995). According to this scheme, radio galaxies, lobe-dominated quasars, and core-dominated quasars are one and the same type of object but seen under different aspect angles. If seen edge-on, a dusty torus obscures the optical nucleus and the quasar is classified as a radio galaxy. For intermediate aspect angles, the optical nucleus, lobes and radio core are visible to give a lobe-dominated radio-loud quasars, and for face-on orientation, relativistic boosting leads to the appearance of a core-dominated quasar, where the core is much brighter than the lobes. A simple tool to separate core and lobe-dominated quasars is the radio spectral index. Radio cores have a flat and variable radio spectrum, while the lobes have a steep spectrum and are not variable.

The unified scheme proved to be very successful and should, in principle, explain the radio properties of all radio-loud quasars. However, it is not clear what radio-loud and radio-weak precisely means. For this purpose Kellermann et al. (1989, hereinafter K89) defined the R-parameter as the ratio between optical flux at 4400Å and radio flux density at 5 GHz and took $R = 10$ as the dividing line between radio-loud and radio-weak quasars (see also K94). But as shown below this value is not necessarily the best choice and is to some degree rather arbitrary.

For their study of the differences between radio-loud and radio-weak quasars, K89 and K94 used the PG quasar sample (Schmidt & Green 1983), which is optically selected and widely studied at almost all wavelengths. Falcke, Malkan, & Biermann (1995; hereinafter FMB95) used the same sample and plotted the radio luminosity against the total UV-bump luminosity (Fig. 2 in FMB95). This diagram allows to consider the absolute luminosity in addition to just the R-parameter and highlights several things: first of all, one finds again a separation of the two radio-loud and radio-weak populations, but there also are a few sources which seem to be intermediate between these two classes. FMB95 identified three sources from the low-redshift part of the PG quasar sample which apparently were separated from the other quasars and labeled them radio-intermediate quasars (RIQ, see also Miller et al. 1993). What made these sources so interesting was the fact that all three were apparently compact, variable, flat-spectrum sources. This would have suggested that they should be relativistically boosted radio-loud quasars. However, their ratio between radio and UV-bump luminosity was equal or even lower than that of a typical lobe-dominated quasar − in marked contrast to what one expects from the unified scheme. These sources also populated the luminosity regime $L_{\rm UV} < 10^{46}$ erg/sec where no steep-spectrum radio-loud quasars are found. The suggestion FMB95 made was that these sources are, in fact, boosted radio-weak quasars. However, it could not be excluded that they are some rare, compact low-power radio-loud sources.

The small number of sources, which was in part due to the lack of radio spectral information for most of the PG quasars, prevented further conclusions. Particularly for radio-weak and radio-intermediate quasars only very few studies of their radio-spectra have been published (see Barvainis, Lonsdale, & Antonucci 1996). We have therefore embarked on a study to investigate the properties of the RIQ in the PG quasar sample in more detail.

In this paper, we report quasi-simultaneous 2.7 GHz and 10.45 GHz flux density measurements using the 100-m telescope at Effelsberg. These observations are used to determine the spectral indices and the variability of the PG quasars in order to identify other flat-spectrum RIQ. In Sec. 2, we describe the

[1] Initially this term was used only for radio emitting quasi-stellar objects (QSOs), but as it is commonly done today, we will use the term 'quasar' for all QSOs

observations and present the results in Section 3. Section 4 discusses the distribution of the R-parameters of the PG quasars in light of the new results and a summary of the paper is given in Section 5.

2. Observations

2.1. Description of the observation

The observations were performed with the MPIfR 100-m telescope in Effelsberg on four different sessions between June 26 to June 30, 1995. The first three nights were divided more or less equally between 2.7 and 10.45 GHz. The fourth night was spent exclusively at 10.45 GHz. Observations and data reduction were performed in a manner as described in Neumann et al. (1994). We used the 11cm (2.695 GHz) and 2.8cm (10.45 GHz) receivers in the secondary focus. These receivers can be switched within a few seconds allowing quasi-simultaneous observations. Other receivers were not available during our observations. We made between 4 and 64 cross-scans for each program source per frequency depending on the expected flux density of the source. On each session we observed 3C286 several times as our primary flux calibrator. Pointing of the telescope was frequently monitored using nearby strong radio point sources. We had clear weather conditions throughout the observations. Several sources were observed at each day to look for possible intraday variability. Data reduction was done using standard MPIfR Toolbox software (von Kap-herr 1980).

2.2. Data Reduction

The flux densities were scaled to the scale of Ott et al. (1994) which supersedes the scale by Baars et al. (1977) and corrected with an elevation dependent gain curve of the telescope. The fluxes given for each source are time averaged fluxes of all scans from the four sessions, which were, however, all calibrated separately. We determined the spectral index α (defined as $F_\nu \propto \nu^\alpha$) from our measured flux densities at 2.7 and 10.45 GHz. Using the above α we calculated an interpolated flux density at 4.9 GHz, which can be used to check the variability with respect to the results of K89 — provided the quasars have a straight spectrum. We estimate that our calibration error is roughly 5% for the brighter sources plus a statistical error (noise) of typically 2 mJy, depending on the number of scans. The final error we give in Table 1 is the combination of statistical and calibration errors; at 2.7 GHz we are confusion limited.

3. Results

3.1. The Effelsberg PG sample

The sample we have observed was basically selected to include PG quasars with flux densities $\gtrsim 4$ mJy at 4.9 GHz and incomplete spectral informations. We did not observe some of the well known radio-loud quasars like e.g. 3C273 (PG 1226+023). Our final sample contained all PG quasars with $1 < R < 150$ (K89) including PG 0003+19 and PG 0007+10 (III Zw 2). The results are summarized in Table 1, where we give the radio flux densities for the observed PG quasars. None of the sources showed intraday variability. We therefore consider only the flux densities averaged over the entire observing period and the spectral indices derived from these.

The reliability of our measurements can be determined by comparing the interpolated fluxes of the 4 steep-spectrum sources (PG 0044+03, PG 0157+00, PG 1241+17, PG 1700+51), which are not expected to be variable, with the VLA fluxes of K89. Within our errors, the measurements agree with each other.

3.1.1. Spectral Indices

Out of the 21 sources, we detected 14 at 2.7 GHz and 17 at 10 GHz. Out of the 13 sources detected at both frequencies 6 have flat or inverted radio spectra ($\alpha > -0.5$) between 2.7 and 10.45 GHz (PG 0007+10, PG 1309+35, PG 1333+17, PG 1538+47, PG 1718+48, PG 2209+18) and 6 have steep spectra (PG 0044+03, PG 0157+00, PG 1241+17, PG 1351+64, PG 1407+26, PG 1700+51). One source (PG 1222+22) has $\alpha \sim -0.5$, but due to the high flux density errors the spectral index is highly uncertain. This means that the fraction of flat-spectrum sources in the Effelsberg PG sample is fairly high — at least 30%. Three of these flat-spectrum sources had simultaneous spectral indices with $\alpha > 0.33$ indicating synchrotron self-absorption. These results are in agreement with the predictions of FMB95 which implied the presence of a substantial fraction of flat-spectrum sources with intermediate radio flux densities.

3.1.2. Variability

We can compare our interpolated 4.9 GHz flux densities with the K89 VLA data and find significant discrepancies for 6 sources — these are basically all the flat spectrum sources except PG 1333+17 but include PG 1222+22, which may also have a flat spectrum. Those discrepancies indicate either variability or a more complex spectral shape — or both.

PG 0007+10 is well known as a violently variable source (e.g. Teräsranta et al. 1992). Comparison of our 10.45 GHz data with those of Neumann et al. (1994) shows that PG 1718+48 and PG 1538+47[2] are variable sources. In addition, comparing the K89 VLA 4.9 GHz data with literature values, we find that also PG 1309+335 (Becker et al. 1991), PG 2209+18 (see Machalski & Magdziarz 1993), and PG1222-22 (Barvainis et al. 1996) show variability. The latter authors also find clear evidence for variability in PG 1216+06, PG 1407+26, and PG 1416-12. Hence, at least 9 out of 21 sources in the Effelsberg PG sample show variability, indicating the presence of strong compact cores at parsec scales. The flux of PG 1351+640 had declined in the past (Barvainis & Antonucci 1989), but now seems to have stabilized at a lower flux-level with a fairly steep spectrum.

3.2. The whole PG sample

We have supplemented the K89 radio data with our data and data from the literature (Barvainis & Antonucci 1989, Barvainis et al. 1996, Neumann et al. 1994, and the NED database, see Falcke 1994). This gives us spectral informations for all PG quasars down to an R-parameter of 1 (i.e. 31 out of 113 sources). In total we have spectral information for 49 sources. Table 2 shows the up-to-date data list. Since the various observations were done in different epochs, some sources can have erroneous spectral indices, due to variability.

As in FMB95, we have averaged the logarithmic flux densities at each frequency, if multiple observations were available, and fitted a power law to the data. Taking the geometric mean is more robust against strong outbursts and the variability in some of the sources, moreover will we later mainly deal with the logarithms of the fluxes. Where appropriate, we fitted 2nd or 3rd order polynomials to the spectra in the log-log plane. Column 2 in Table 2 gives the flux density at 4.9 GHz from those fits for all sources. For sources with only one datapoint at 4.9 GHz we give this value. We also tabulated the optical flux from K89, the estimated UV-bump luminosity from FMB95 and the differential spectral index α at 4.9 GHz where available. The latter is defined as the slope of the tangential to the fitted spectra at 4.9 GHz.

Since our time averaged flux densities differ slightly from K89 we recalculated the R-parameter, which is the ratio between Col. 2 and 3 of Table 2, but also give the old K89 value (here $R_{\rm K94}$). Moreover, we also defined a new parameter $R_{\rm UV}$, which is the ratio between the monochromatic radio luminosity at 5 GHz in the rest-frame and the UV-bump luminosity ($L_{\rm disk}$) divided by $\nu = 1.5 \cdot 10^{15}$Hz, which corresponds to a wavelength of 2000Å. The wavelength was chosen such that $R_{\rm UV}$ has values roughly similar to R, thus allowing an easy comparison between the FMB95 and K89 methods of organizing the data in the optical/radio plane.

Comparison of Col. 6 with Col. 7 & 8 shows that all three definitions of the R-parameter yield consistent results, with the exception of a few high-redshift sources where $R_{\rm UV}$ is smaller than R. In order to make comparisons with other data sets easier, we use here the radio/optical R-parameter in the observers frame for our discussion of the radio properties of the PG quasars (Col. 7). As shown above, taking absolute luminosities rather than fluxes would not have changed our results significantly, that might, however, change for a high-redshift sample.

4. Distribution of the R-parameter

4.1. What is radio-loud?

In the PG quasar sample, 96 out of 113 sources (85%) have a well defined R-parameter and only 17 have upper limits. Those upper limits concern only the part of the sample where $R \lesssim 0.1$. Since we concentrate on the regime $R > 0.1$ we will not explicitly separate the upper limits from the detections. In Fig. 1a, we show a histogram of the distribution of R-parameters for the PG quasars in logarithmic intervals.

First of all, the bimodal distribution, which corresponds to the radio-loud/radio-weak dichotomy is apparent and it is quite obvious that radio-weak quasars cluster around R=0.2, while radio-loud quasars clus-

[2] Note that PG 1538+47 was classified as a steep-spectrum source in FMB95, due to a non-simultaneous flux measurement (White & Becker 1992).

ter around R=300. Nonetheless, there are quite a few sources in between the distributions, where radio-loud and radio-weak quasars seem to blend into each other, and it is not clear how far the tails of both distributions reach. The classification of a quasar as radio-loud or radio-weak is, therefore, somewhat ambiguous in the range R=10-50. If, on the other hand, one considers only the steep-spectrum sources as shown in Fig. 1b, the two distributions are much better separated. The reason for this ambiguity is the presence of a strong population of flat-spectrum radio-intermediate quasars: six out of thirteen quasars with $3 > R > 200$ have a flat radio spectrum. A similar trend was found from the Effelsberg PG sample alone. K94 showed that all these flat-spectrum radio-intermediate quasars are compact on the VLA scale.

4.2. Conflict with the unified scheme

Taking $R = 10$ as the dividing line between radio-loud quasars and radio-weak quasars we have 22 radio-loud quasars in the total sample of 113 quasars (19%) and 9 out of these 22 radio-loud quasars are flat-spectrum sources (41%). This number is surprisingly high and difficult to reconcile with the standard unified scheme for core- and lobe-dominated sources. For a randomly oriented sample with N quasars which have an obscuring torus with semi-opening angle $\phi_{\rm opening}$ and an average bulk Lorentz factor of $\gamma_{\rm jet}$ one finds that

$$n = N(1 - \sqrt{1 - \gamma_{\rm jet}^{-2}})/(1 - \cos\phi_{\rm opening}) \qquad (1)$$

objects should be flat-spectrum sources assuming that objects with inclination $i \leq \arcsin\gamma_{\rm jet}^{-1}$ are core-dominated.

For $\phi_{\rm opening} = 60^\circ$ and $\gamma_{\rm jet} = 3$ one expects only 10% flat-spectrum sources, while a 40% fraction would indicate a Lorentz factor as low as $\gamma_{\rm jet} \simeq 1.6$. On the other hand, for a source with $i = \gamma_{\rm jet}^{-1}$ the Doppler enhancement of the flat-spectrum core is at best γ^3. As the cores of steep-spectrum radio-loud quasars are usually only 10% or less of the lobe luminosity at 4.9 GHz we would need at least a 30-fold enhancement of the core flux density, hence a Lorentz factor $\gamma_{\rm jet} \gtrsim 3$ for a radio-loud quasar to become core-dominated.

Besides the number of sources, also the distribution of R-parameters for the flat-spectrum sources is completely inconsistent with the simple unified scheme. Obviously, core-dominated sources can only be core-dominated as long as the core is substantially brighter than the radio lobes. Since the lobes are expected to radiate largely isotropically the median R-parameter of the flat-spectrum radio-loud quasars should always be equal or larger than the ones of the steep-spectrum radio-loud quasars. This remains true even if there is some beaming in the optical spectrum. First of all, the optical emission would at best be boosted by the same amount as the radio emission and secondly, the optical and UV spectrum of the flat-spectrum PG quasars indicate that the enhancement of the optical flux due to a possible beamed component is still relatively modest. For example, 3C273, the source with the strongest non-thermal beamed component, has still the largest R-parameter in the sample.

In marked contrast to the expectations, the median R-parameter for the steep-spectrum radio-loud quasars is 217, while for the flat-spectrum radio-loud quasars it is only 94. This again is due to the large population of flat-spectrum radio-intermediate quasars that cluster below the peak of the steep-spectrum distribution. Only 2 flat-spectrum radio-loud quasars, PG1226+02 (3C273) and PG 2344+09, are above the median steep-spectrum R-parameter. Interestingly, only these sources occur in the right number and have R-parameters expected from the unified scheme.

In summary, if one uses $R = 10$ as the boundary between radio-loud and radio-weak quasars, the contents of the PG quasar sample clearly contradicts the unified scheme. There are too many flat-spectrum sources and they have on average a radio luminosity which is too low compared with their optical luminosity.

4.3. Effects of a radio-selected sample

One of the advantages of the PG quasar sample is that it is optically selected and the radio flux densities range from several Janskys to a fraction of milli-Jansky. The conclusions of the above section would be strongly altered if only a radio-selected sample is used. Typical radio samples have a flux density cut-off of the order 1 Jy, some deeper wide-field radio surveys go down to 200 mJy (e.g. Patnaik et al. 1992), however, most of the flat-spectrum radio-loud quasars in the PG quasar sample have flux densities < 200 mJy. If we would impose a radio flux density limit of 200 mJy for the PG quasars we would be left with only 2 flat-spectrum and 7 steep-spectrum quasars. The median R-parameters for these few sources are 1100 and 360

respectively, in reasonable agreement with the predictions of the unified scheme. This limit is only a technical one, but illustrates how the conclusions can be biased if the sample is radio-selected.

4.4. Are there boosted radio-weak quasars?

One can now ask the question, if it is possible to interpret our data in a way that is consistent with the unified scheme rather than contradicts it? The clue to this answer lies in the distribution of flat-spectrum sources themselves. As mentioned above, there does not appear to be any problem with the unified scheme for the the high radio flux source (i.e. high R sources), only the flat-spectrum sources with $R \lesssim 150$ are difficult to reconcile, because of the presence of the flat-spectrum radio-intermediate quasars. This means that in order to reconcile our data with the unified scheme, we have to give a reasonable explanation for the nature of the flat-spectrum radio-intermediate quasars.

A common feature of these sources is that they have flat spectra, are compact and are variable. This are typical characteristics of radio cores in radio-loud quasars. However, the low R and the correspondingly low limit on the extended, steep-spectrum emission is untypical for radio-loud quasars. Their variability and their often inverted spectra argue against Gigahertz-Peaked-Spectrum (GPS) and Compact-Steep-Spectrum (CSS) sources, supernovae or free-free emission as an explanation. Their relatively large number with respect to radio-loud quasars also argues against some kind of exotic, naked radio-loud quasars without radio lobes.

One viable explanation for the flat-spectrum radio-intermediate quasars, however, is that, just like radio-loud quasars, radio-weak quasars are subject to relativistic boosting and orientation effects. In this case the flat-spectrum radio-intermediate quasars were just the boosted radio-weak quasars and one would have two separate bi-modal distributions for flat- and steep-spectrum quasars, so that boosted, flat-spectrum radio-weak quasars and unboosted, steep-spectrum radio-loud quasars would blend into each other, when considering only the R parameter. A proper classification of radio-loud and radio-weak quasars would then require to take R *and* α into account.

In fact, classification of radio-loud and radio-weak quasars can be considerably improved in the regime $1 < R < 300$ if we consider steep- and flat-spectrum sources separately. As shown in Fig. 1b a limiting value of $R \sim 25$ would effectively separate the radio-loud and the radio-weak distributions of the steep-spectrum quasars[3]. Only one source, PG 0044+03, a compact steep-spectrum source with $R \simeq 25$ would remain ambiguous. All other steep-spectrum radio-loud quasars do not only seem to belong to the same distribution, but also have very similar radio morphologies (K94), i.e. they are all edge-brightened FR-II like radio sources[4]. The median R-parameters would then be $\langle R \rangle = 0.2$ for steep-spectrum radio-weak quasars and $\langle R \rangle = 240$ for steep-spectrum radio-loud quasars.

The flat-spectrum sources are more difficult to classify as their number is much lower. Since treating them as a single class leads to severe inconsistencies with the unified scheme, we will make the assumption that their distribution is bi-modal as well and shifted by relativistic boosting to higher R parameters. This implies that we assume that radio-weak quasars also have relativistic jets in their cores, which are just a factor $\sim 100 - 1000$ less luminous than in radio-loud quasars and if pointed towards us appear as flat-spectrum radio-intermediate quasars. Unfortunately, because of the small sample, we cannot determine the dividing line between radio-loud and radio-weak flat-spectrum sources from Fig. 2a directly; we therefore have to guess.

For example, if we adopt $R = 250$, which is just above the median step-spectrum value, as the dividing R-parameter between the two putative flat-spectrum distributions, the situation would change quite significantly. Only 2 flat-spectrum sources would be considered as radio-loud, while 10 flat-spectrum radio-intermediate quasars sources in the range $1 < R < 250$ would be considered radio-weak. The median values for these two populations are $\langle R \rangle = 1130$ and $\langle R \rangle = 20$ respectively. The median R-parameter for the putative radio-weak flat-spectrum sources is, however, biased because we only have complete spectral informations down to $R = 1$; for example, the me-

[3] Here we call the radio-weak quasars with low R and without spectral information also "steep-spectrum" quasars even though their spectral index is not properly known. At least that we consider them to be the equivalents to steep-spectrum radio-loud quasars in the unified scheme, i.e. sources which are not preferentially oriented and which make up the bulk of the parent population.

[4] PG 1241+17 may be a possible exception as it has one very bright, steep-spectrum component that is connected to a second weaker component by a bridge — it may also be a second, peculiar CSS quasar.

dian R-parameter for all flat-spectrum sources with $R < 250$ would be only $\langle R \rangle = 6.5$. It is of course possible that there are more flat-spectrum sources at lower R which have not been observed, thus lowering $\langle R \rangle$ even further. On the other hand the limit $R = 1$ is reasonable as it separates the bulk of the radio-weak quasars distribution from the radio-intermediate quasars. It may be that the spectral index of radio-weak quasars is affected by free-free emission in the nucleus at low values of R. Another possible pitfall is that the extended emission of radio-weak quasars is relatively weaker than in radio-loud quasars compared to their radio cores and therefore even for larger inclinations the core still dominates.

Anyhow, even if the assumption of a bi-modal distribution of flat-spectrum quasars cannot yet be statistically proven, it is consistent with our data and gives a much more satisfying interpretation of it. The small number of *radio-loud* flat-spectrum (14%) sources is now in agreement with the predictions of the unified scheme and Lorentz factors of $\gamma_{\rm jet} = 2-4$. The ratio between the median R-parameters for flat- and steep-spectrum radio-loud quasars is ~ 5, which implies a relativistic boosting by a factor 50 for typical core luminosities of 10% of the total flux in steep-spectrum radio-loud quasars. This is consistent with the range of Lorentz factors mentioned above.

Moreover, with the above classification, we have a fraction of 10% flat-spectrum radio-weak quasars with $R > 1$ and a ratio of 30-100 between median radio-weak flat- and steep-spectrum R-parameters. As the core fraction in radio-weak quasars is on average much higher than in radio-loud quasars (i.e. ~ 0.8, K89) the enhancement factors and the fraction of flat-spectrum radio-weak quasars are very similar to those of the flat-spectrum radio-loud quasars and hence also consistent with Lorentz factors of 2-4.

5. Discussion and Summary

We have measured quasi-simultaneous spectral indices for PG quasars with intermediate radio luminosities and typical flux densities of 4-200 mJy. We find that a substantial fraction of these sources are flat-spectrum sources and are variable. Six out of 13 quasars with radio-to-optical ratios of $3 > R > 200$ are compact flat-spectrum radio quasars and constitute a population of flat-spectrum radio-intermediate quasars (RIQ). This confirms an earlier prediction for the radio-intermediate quasars by FMB95 which was based on a subsample of the PG quasars.

Together with data from the literature we have now almost complete spectral information for PG quasars down to $R \sim 1$. If one uses the definition for a radio-loud source of $R > 10$ (K89) we find severe inconsistencies in the content of the PG quasar sample with the simple unified scheme. According to the unified scheme flat-spectrum, core-dominated sources are the relativistically boosted counterparts to steep-spectrum, lobe-dominated sources. Therefore, they should be rare and they should have higher radio flux densities than steep-spectrum sources. However, if we treat the flat-spectrum quasars as a single population, the flat-spectrum sources are quite frequent (40%) in the PG sample and the majority has lower flux densities and lower R-parameters than steep-spectrum quasars. Under these prerequisites our observations exclude that core-dominated quasars are generally the boosted counterparts of *lobe-dominated, steep-spectrum radio-loud quasars*.

We point out that this problem can be easily circumvented if one assumes that the distributions of flat- and steep-spectrum quasars are both bi-modal. In this case one would separate radio-loud and radio-weak steep-spectrum sources at $R \simeq 25$ and radio-loud and radio-weak flat-spectrum quasars at a higher value of $R \sim 250$, where the latter number is fairly uncertain due to the small number of flat-spectrum quasars. As a consequence, the fraction of flat-spectrum quasars would be only of the order 10% for *both*, radio-loud and radio-weak quasars. This fraction of flat-spectrum sources as well as the relative enhancement of the radio cores in radio-loud and radio-weak quasars between flat- and steep-spectrum sources is consistent with average Lorentz factors of $2-4$ and now fits well into the unified scheme for radio-loud quasars.

The implication of this suggestion is that radio-weak quasars are as much subject to relativistic boosting as are radio-loud quasars, and the flat-spectrum radio-intermediate quasars are just the boosted counterparts to radio-weak quasars — this agrees well with the jet-disk symbiosis idea for radio-weak and radio-loud quasars proposed by Falcke & Biermann 1995 and FMB95, which postulates that the central engines in quasars produce initially very similar radio jets. It is known, that a large fraction of Seyfert galaxies, which are believed to be the low-power counterparts to quasars, have collimated bi-polar radio outflows (Ulvestad & Wilson 1989). Radio morphological stud-

ies of radio-weak quasars also show evidence of jet-related structures (K89). Hence it is not surprising to find jets in radio-weak quasars. However, so far no Seyfert galaxy has shown evidence for relativistic motion in its radio jets (although this is not yet excluded for the cores). Therefore, the flat-spectrum radio-intermediate quasars could be an important clue for the understanding of jets in radio-weak sources. It may, for example, be that the jet speed is somehow related to the total luminosity or to the Eddington luminosity of the central engine and becomes relativistic only for high-power engines.

There are also a few other arguments that support the link between the radio-weak quasars and the flat-spectrum radio-intermediate quasars. While the radio-weak quasars in the PG sample have absolute UV luminosities that stretch from 10^{44}erg/sec to 10^{48}erg/sec, steep-spectrum radio-loud quasars are only found only in the interval 10^{46}erg/sec$< L <$ 10^{48}erg/sec (Falcke, Gopal-Krishna, & Biermann 1995). As one can infer from FMB95, the low-redshift flat-spectrum radio-intermediate quasars do indeed have lower absolute powers, than the weakest steep-spectrum radio-loud quasars. With the identification of the new, high-z flat-spectrum radio-intermediate quasars, the flat-spectrum radio-intermediate quasars now also stretch over the whole luminosity range, just like the radio-weak quasars. Another indirect clue comes from spectroscopic observations of $z < 0.5$ PG quasars. Boroson & Green (1992) found that radio-weak quasars have stronger Fe II emission than radio-loud quasars (which they define to be at $R > 1$), but they also point out that core-dominated radio-loud quasars too have relatively strong Fe II, moving them closer to radio-weak quasars. We note that 4 of their core-dominated 5 sources are flat-spectrum radio-intermediate quasars and hence might be boosted radio-weak quasars.

Our interpretation can be tested further by VLBI observations of the flat-spectrum radio-intermediate quasars and studies of their host galaxies. One would expect to see a very compact nucleus in these sources, and possibly core-jet structures and superluminal motion as seen in many lobe- and core-dominated radio-loud quasars (e.g. Hough et al. 1992 and Zensus, Cohen, & Unwin 1995). However, if the flat-spectrum radio-intermediate quasars are indeed radio-weak quasars, one expects the limits for the resolved, and extended emission (i.e. radio lobes) to be very low, with fluxes corresponding to R-parameters of unity or less. This is in marked contrast to what one expects to see for a boosted radio-loud quasar and is a testable prediction. Moreover, as the host-galaxies are markedly different between radio-loud and radio-weak quasars one expects to find a substantial fraction of spiral host galaxies for the flat-spectrum radio-intermediate quasars. We also need a larger optically selected quasar sample with deep VLA observations and quasi-simultaneous flux-measurements to directly prove the bi-modality of flat-spectrum quasars. If these tests fail, the flat-spectrum radio-intermediate quasars would constitute a major puzzle for our understanding of the radio properties of quasars and one would have to invoke other, possibly more exotic explanations for the flat-spectrum radio-intermediate quasars.

Finally we wish to point out that without spectral information the flat-spectrum radio-intermediate quasars can spoil all studies concerned with the radio properties of quasars and the difference between radio-loud and radio-weak quasars. At least in an optically selected sample one would simply overestimate the number of radio-loud sources in certain regimes. This is especially critical for the determination of the paucity of radio-loud quasars found at low powers (see Falcke et al. 1995b), where some flat-spectrum radio-intermediate quasars could be falsely classified as radio-loud quasars.

During the preparation of this manuscript we have learned that similar observations with very similar results had been performed by H. Steppe and his collaborators. Due to the early death of the PI these results have not yet been published. We thank P. Strittmatter for bringing this to our attention. We also thank H. Teräsranta for some more information and unpublished data on the variability of III Zw 2, we are grateful to Jürgen Neidhöfer and Alex von Kap-herr for their friendly support and to an anonymous referee for several suggestions and comments. This research was supported in part by NASA under grants NAGW-3268 and NAG8-1027.

Table 1

Radio flux densities and spectral indices from Effelsberg observations

Name	2.7 GHz mJy		10.45 GHz mJy		4.9 GHz interp	4.9 GHz VLA	$\alpha_{2.7}^{5}$	$\alpha_{2.7}^{10}$ Eff.	α_{5}^{10}
PG 0003+19	<10		3	±2		3.9	>−1.6	>−0.89	−0.35
PG 0007+10	102	±5.5	617	±31.	(230.)	321	1.9	1.3	0.86
PG 0026+12	<10		<4			5.1	>−1.1		<−0.32
PG 0044+03	78	±4.4	19	±2.6	(42.)	38	−1.2	−1.	−0.92
PG 0157+00	17	±2.2	4	±2	(9.)	8	−1.3	−1.1	−0.92
PG 0921+52	8	±4	<4			3.8	−1.2	<−0.51	<0.068
PG 0923+12			3	±2		10			−1.6
PG 1216+06	<10		3	±2		4	>−1.5	>−0.89	−0.38
PG 1222+22	8	±3	4	±4	(5.9)	12.	0.65	−0.51	−1.4
PG 1241+17	306	±15.	88	±4.7	(180.)	180	−0.89	−0.92	−0.94
PG 1309+35	30	±2.5	30	±2.6	(30.)	54	0.99	0	−0.78
PG 1333+17	32	±2.6	21	±2.4	(27.)	25	−0.41	−0.31	−0.23
PG 1351+64	24	±2.3	5	±2	(12.)	13.	−0.99	−1.2	−1.3
PG 1407+26	12	±2.1	4	±2	(7.4)	7.9	−0.69	−0.81	−0.91
PG 1416−12	<10		<6			3.6	>−1.7		<0.67
PG 1538+47	49	±3.2	63	±3.9	(55.)	26	−1.1	0.19	1.2
PG 1612+26	<10		3	±1		5.1	>−1.1	>−0.89	−0.69
PG 1613+65	<10		<4			3	>−2.		<0.38
PG 1700+51	15	±2.1	5	±2	(9.2)	7.2	−1.2	−0.81	−0.48
PG 1718+48	112	±5.9	217	±11.	(150.)	137	0.34	0.49	0.61
PG 2209+18	164	±164	261	±13.	(200.)	113	−0.62	0.34	1.1

Note.—Flux densities and spectral indices of PG quasars as measured with the Effelsberg 100m telescope and the VLA (Kellermann et al. 1994). All flux densities are in mJy. Description of columns: (1) – Name of source in PG sample, (2) – Effelsberg 2.7 GHz flux, (3) – Effelsberg 10.45 GHz flux, (4) – interpolated Effelsberg 4.9 GHz flux, (5) – VLA 4.9 GHz flux, (6-8) – spectral indices for 2.7/5, 2.7/10, and 5/10.45 GHz (only $\alpha_{2.7}^{10}$ is simultaneous).

Table 2
Radio Properties of PG Quasars

Name	S_ν(4.9 GHz)/mJy	S_o/mJy	$\lg L_{\rm disk}$	$\alpha_{\rm 5GHz}$	$R_{\rm UV}$	R	$R_{\rm K94}$
0003+15	332.6	1.87	46.4	−0.8	143.	178.	175.
0003+19	3.92	14.3	44.6	−0.36	0.4	0.3	0.3
0007+10	257.6	1.63	45.4	0.66	45.2	158.	197.
0026+12	5.1	4.74	45.5	···	1.7	1.1	1.1
0043+03	0.24	2.01	46.	···	0.2	0.1	0.1
0044+03	44.82	1.85	46.5	−1.	25.5	24.2	20.5
0049+17	0.64	2.01	44.6	···	0.4	0.3	0.3
0050+12	2.43	7.94	45.	−0.77	0.5	0.3	0.3
0052+25	0.74	3.08	45.6	···	0.2	0.2	0.2
0117+21	0.25	1.72	47.2	···	0.1	0.1	0.2
0157+00	7.55	3.77	45.6	−1.	3.	2.	2.1
0804+76	1.29	3.94	45.4	−0.58	0.3	0.3	0.6
0838+77	<0.15	1.37	45.	···	<0.1	<0.1	0.1
0844+34	0.31	11.4	44.9	···	0.1	0.	0.
0921+52	3.8	2.56	44.5	−1.2	1.	1.5	1.5
0923+12	10.	4.83	44.3	−1.6	2.5	2.1	2.1
0923+20	0.25	1.74	45.6	···	0.1	0.1	0.1
0934+01	0.53	1.38	44.3	···	0.4	0.4	0.4
0946+30	<0.15	1.8	47.1	···	<0.	<0.1	<0.1
0947+39	0.31	1.25	45.3	···	0.3	0.2	0.3
0953+41	1.9	4.33	46.1	···	0.5	0.4	0.4
1001+05	0.8	1.6	45.2	···	0.8	0.5	0.5
1004+13	417.9	1.92	45.8	−1.	225.	218.	228.
1008+13	<0.15	1.45	47.7	···	<0.	<0.1	<0.2
1011−04	0.28	2.88	44.6	···	0.2	0.1	0.1
1012+00	1.17	2.	45.5	−0.56	0.6	0.6	0.5
1022+51	0.37	1.61	44.1	···	0.4	0.2	0.2
1048+34	<0.21	2.15	45.4	···	<0.1	<0.1	0.1
1048−09	653.5	1.8	45.9	−0.88	494.	363.	377.
1049−00	0.48	1.89	46.2	···	0.2	0.3	0.3
1100+77	660.	2.05	46.	−0.99	362.	322.	322.
1103−00	461.9	1.77	45.9	−0.55	476.	261.	272.
1114+44	0.22	1.72	45.3	···	0.1	0.1	0.1
1115+08	<0.15	2.09	47.6	···	<0.	<0.1	<0.1
1115+40	0.3	1.77	45.1	···	0.3	0.2	0.2
1116+21	1.97	3.87	45.9	−0.79	0.5	0.5	0.7
1119+12	0.94	6.25	44.6	···	0.3	0.2	0.2
1121+42	<0.18	1.77	45.4	···	<0.2	<0.1	0.1
1126−04	0.51	3.05	44.9	···	0.1	0.2	0.2
1138+04	<0.15	1.72	47.4	···	<0.	<0.1	4.8
1148+54	1.47	2.13	47.1	−0.92	0.4	0.7	0.6
1149−11	2.6	2.96	44.6	···	0.9	0.9	0.9
1151+11	<0.2	2.83	45.4	···	<0.1	<0.1	<0.1
1202+28	0.83	4.45	45.4	···	0.5	0.2	0.2
1206+45	<0.12	2.19	47.1	···	<0.	<0.1	<0.1
1211+14	0.83	6.37	45.5	···	0.1	0.1	0.1
1216+06	5.97	2.42	46.1	0.29	2.1	2.5	1.7
1222+22	6.07	2.88	47.5	−0.31	1.2	2.1	4.1
1226+02	43850.	32.5	46.5	−0.085	1810.	1350.	1138.
1229+20	0.67	6.25	44.9	···	0.2	0.1	0.1
1241+17	180.9	3.19	47.2	−0.77	59.9	56.7	56.4
1244+02	0.83	1.57	44.1	···	0.9	0.5	0.5
1247+26	1.	2.78	47.8	···	0.1	0.4	0.4
1248+40	<0.15	1.71	46.9	···	<0.1	<0.1	<0.1
1254+04	0.27	2.09	47.	···	0.1	0.1	0.1
1259+59	<0.15	2.16	46.3	···	<0.1	<0.1	<0.1
1302−10	913.8	4.17	45.9	0.035	385.	219.	187.

Table 2—*Continued*

Name	S_ν(4.9 GHz)/mJy	S_o/mJy	lg L_{disk}	α_{5GHz}	R_{UV}	R	R_{K94}
1307+08	0.35	3.5	45.6	···	0.1	0.1	0.1
1309+35	33.76	2.99	45.5	−0.021	16.7	11.3	18.
1310−10	0.26	2.73	44.4	···	0.1	0.1	0.1
1322+65	0.2	2.05	45.2	···	0.2	0.1	0.1
1329+41	0.25	1.37	47.2	···	0.1	0.2	0.2
1333+17	25.93	2.51	46.6	−0.31	8.2	10.3	10.
1338+41	<0.15	1.67	47.3	···	<0.	<0.1	<0.1
1341+25	<0.23	1.92	44.7	···	<0.2	<0.1	0.1
1351+23	0.52	2.03	44.3	···	0.5	0.3	0.3
1351+64	24.15	3.08	45.2	−0.57	6.1	7.8	4.3
1352+01	<0.15	1.75	47.2	···	<0.	<0.1	<0.1
1352+18	0.25	2.36	45.3	···	0.2	0.1	0.1
1354+21	<0.17	2.07	45.5	···	<0.3	<0.1	0.1
1402+26	0.62	2.68	45.3	···	0.5	0.2	0.2
1404+22	0.97	2.13	44.7	−0.93	1.1	0.5	0.5
1407+26	7.04	2.31	47.	−0.32	1.8	3.	3.4
1411+44	0.61	4.57	45.2	···	0.2	0.1	0.1
1415+45	0.4	2.29	44.9	···	0.4	0.2	0.2
1416−12	1.7	3.13	45.4	0.	0.6	0.5	1.1
1425+26	132.8	2.44	46.	−0.75	84.4	54.4	53.6
1426+01	1.14	4.33	45.3	−0.26	0.3	0.3	0.3
1427+48	<0.21	1.33	45.5	···	<0.2	<0.2	0.2
1435−06	0.19	2.75	45.3	···	0.1	0.1	0.1
1440+35	1.15	4.53	44.9	−1.1	0.5	0.3	0.4
1444+40	0.16	1.89	45.6	···	0.1	0.1	0.1
1448+27	1.32	4.49	44.8	−0.6	0.5	0.3	0.3
1501+10	1.5	4.17	45.1	···	0.1	0.4	0.4
1512+37	351.5	1.85	46.1	−0.71	188.	190.	190.
1519+22	1.5	1.66	45.	···	1.5	0.9	0.9
1522+10	0.29	2.29	47.8	···	0.	0.1	0.1
1534+58	1.92	2.75	44.5	···	0.3	0.7	0.7
1535+54	0.47	3.4	44.6	···	0.1	0.1	0.1
1538+47	49.15	1.79	46.7	−0.4	19.6	27.5	14.5
1543+48	1.08	1.72	45.8	−0.89	1.4	0.6	0.6
1545+21	810.9	1.72	45.9	−0.98	432.	471.	418.
1552+08	0.8	1.77	44.8	···	1.	0.5	0.5
1612+26	4.87	1.8	45.7	−1.1	1.	2.7	2.8
1613+65	2.5	3.03	45.4	−0.45	0.9	0.8	1.
1617+17	1.89	2.63	45.2	···	0.9	0.7	0.7
1626+55	0.17	1.54	45.1	···	0.1	0.1	0.1
1630+37	<0.15	1.87	47.4	···	<0.	<0.1	<0.1
1634+70	1.26	4.97	47.9	−0.023	0.	0.3	0.4
1700+51	7.14	3.05	46.	−0.95	3.6	2.3	2.4
1704+60	1194.	1.91	45.9	−0.84	970.	625.	645.
1715+53	0.8	1.37	47.4	···	0.3	0.6	0.6
1718+48	123.4	3.34	47.5	−0.058	8.6	36.9	41.1
2112+05	0.91	2.81	46.5	−0.96	0.3	0.3	0.3
2130+09	2.38	6.43	45.2	−0.51	0.4	0.4	0.3
2209+18	188.1	2.05	44.9	0.32	62.1	91.8	141.
2214+13	0.24	4.61	45.	···	0.1	0.1	0.1
2233+13	0.48	1.74	45.6	···	0.6	0.3	0.3
2251+11	556.8	1.43	46.	−0.72	324.	389.	365.
2302+02	0.36	1.75	47.2	···	0.1	0.2	0.2
2304+04	0.77	3.02	44.4	···	0.3	0.3	0.3
2308+09	224.2	1.61	46.1	−0.89	184.	139.	188.
2344+09	1523.	1.67	46.5	−0.18	793.	912.	1010.

Note.—The columns are (1) – source name, (2) – average radio flux at 5 GHz, (3) – optical flux, (4) – log disk luminosity in erg/sec (FMB95), (5) – spectral index at 5 GHz, (6) – ratio between radio flux and UV flux in rest frame, (7) – ratio between radio flux and optical flux, (8) – same as Col. 7 but for K89 radio data

REFERENCES

Baars, J.W.M., Genzel, R., Pauliny-Toth, I.I.K., & Witzel, A. 1977, 61, 99

Barthel, P.D. 1989, ApJ 336, 606

Barvainis, R., & Antonucci, R. 1989, ApJS 70, 257

Barvainis, R., Lonsdale, C., & Antonucci, R., 1996, AJ, in press

Becker, R.L., White, R.L., & Edwards, A.L. 1991, ApJS 75, 1

Boroson, T.A., & Green, R.F. 1992, ApJS 80, 109

Falcke, H. 1994, PhD Thesis, RFW Universität Bonn

Falcke, H., Mannheim, K., & Biermann, P. L. 1993, A&A 278, L1

Falcke, H., & Biermann, P.L. 1995, A&A 293, 665

Falcke, H., Malkan, M., & Biermann, P.L. 1995a, A&A 298, 375 (FMB95)

Falcke, H., Gopal-Krishna, & Biermann, P.L. 1995b, A&A 298, 395

Hough, D.H., Readhead, A.C.S., Wood, D.A., Feldmeier, J.J., ApJ 393, 81

Kellermann, K.I., Sramek, R., Schmidt, M., Shaffer, D.B., & Green, R. 1989, AJ 98, 1195 (K89)

Kellermann, K.I., Sramek, R., Schmidt, M., Green, R., & Shaffer, D.B. 1995, AJ 108, 1163 (K94)

Miller, P., Rawlings, S., & Saunders, R. 1993a, MNRAS 263, 425 (MRS)

Machalski, J., & Magdziarz, P. 1993, A&A 267, 363

Neumann, M., Reich, W., Fürst, E., Brinkmann W., Reich, P. et al. 1994, A&AS 106, 303

Ott, M., Witzel, A., Quirrenbach, A., Krichbaum, T.P., Standke, K.J., Schalinski, C.J., & Hummel, C.A. 1994, A&A 284, 331

Patnaik, A.R., Browne, I.W.A., Wilkinson, P.N., & Wrobel, J.M. 1992, MNRAS 254, 655

Schmidt, M., & Green, R. 1983, ApJ 269, 352

Strittmatter, P.A., Hill, P., Pauliny-Toth, I.I.K., Steppe, H., & Witzel, A. 1980, A&A 88, L12

Teräsranta, H., Tornikoski, M., Valtaoja, E. et al. 1992, A&AS 94, 121

Ulvestad, J.S. & Wilson, A.S. 1989, ApJ 343, 659

Urry, C.M., & Padovani, P. 1995, PASP 107, 803

von Kap-herr, A. 1980, Technical Report No. 40, MPIfR Bonn, Sept. 1980 (up-dated on-line version)

White, R.L., & Becker, R.H. 1992, ApJS 79, 331

Zensus, J.A., Cohen, M.H., Unwin, S.C. 1995, ApJ 443, 35

This 2-column preprint was prepared with the AAS LaTeX macros v4.0.

Fig. 1.— Distribution of the R-parameter, the ratio between radio and optical flux, for all PG quasars (top) and the steep-spectrum PG quasars (bottom). The labels directly below the bars gives the *upper* cut-off for R for the sources counted in that interval; the lower cut-off is the label to the left. For most of the weak radio sources ($R < 1$) the spectrum is not known and hence they are all marked as 'steep', even though some may have flat spectra. The intervals are logarithmic and upper limits for R (below $R \lesssim 0.15$) are not marked explicitly. The two distributions (radio-loud and radio-weak) are clearly visible, but the dividing line is better defined if one removes the flat-spectrum radio sources.

Fig. 2.— The top panel shows the same as Fig. 1b for the flat-spectrum PG quasars. The bottom panel shows Fig. 1a with the flat-spectrum quasars at $R > 1$ shaded in grey. Obviously a large fraction of the sources intermediate between radio-loud and radio-weak are flat-spectrum sources. Only a minority of two of the flat-spectrum sources are at the upper end of the distribution as expected in the unified scheme.

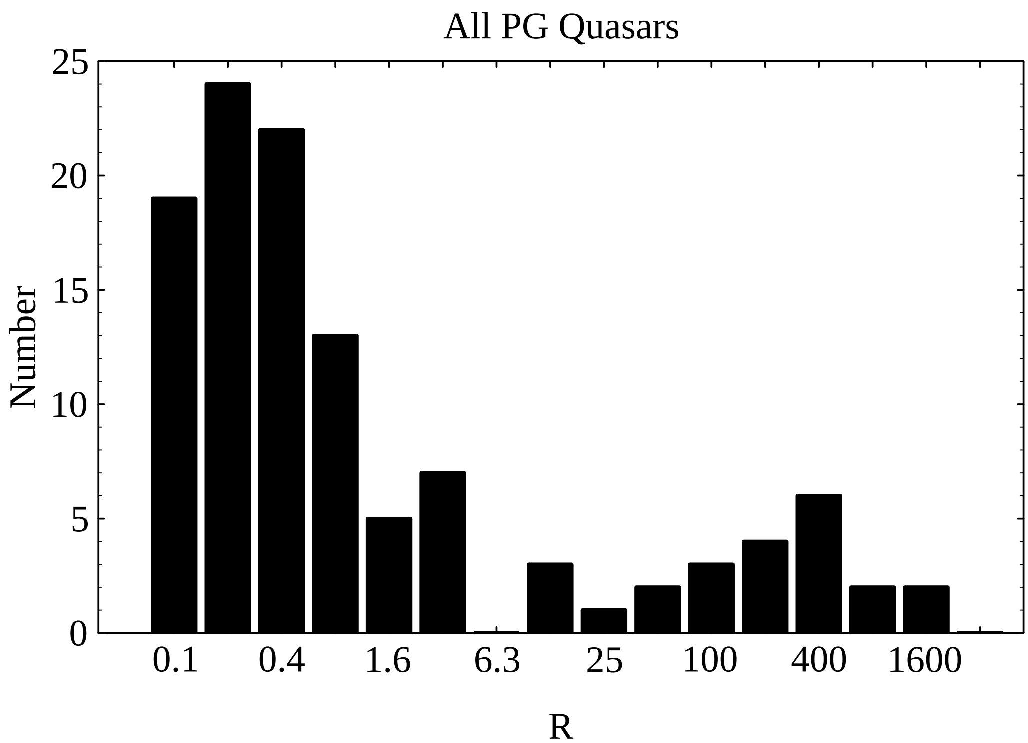

All PG Quasars
Number
25
20
15
10
5
0
0.1
0.4
1.6
6.3
25
100
400
1600
R

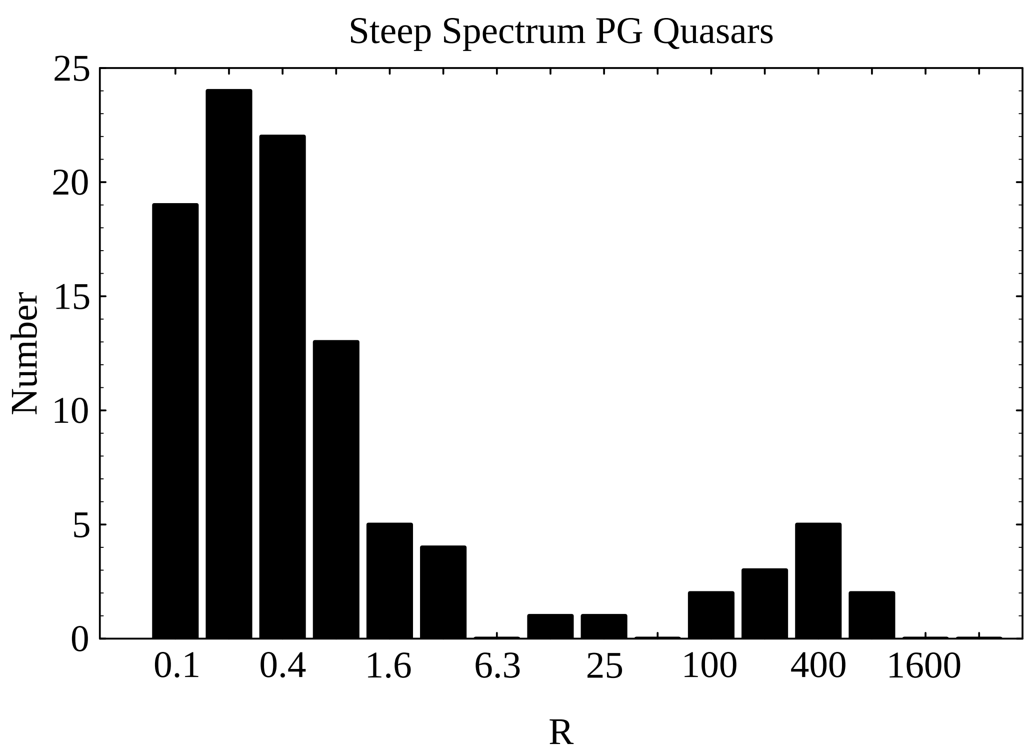

Steep Spectrum PG Quasars
Number
25
20
15
10
5
0
0.1
0.4
1.6
6.3
25
100
400
1600
R

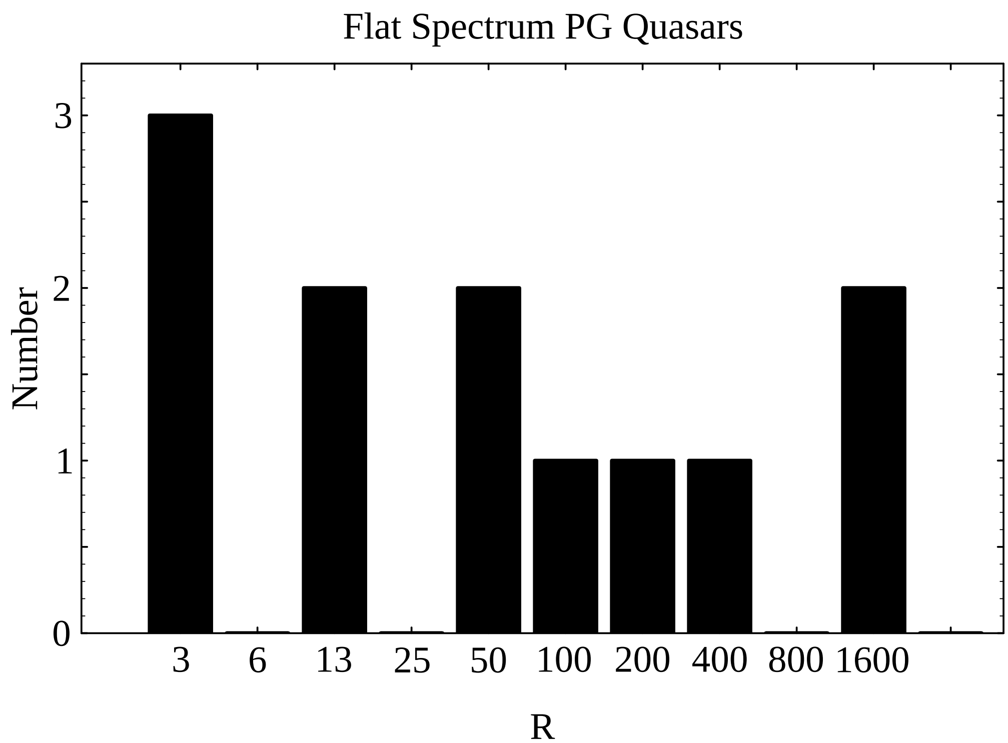
Flat Spectrum PG Quasars
Number
R
3
6
13
25
50
100
200
400
800
1600
0
1
2
3

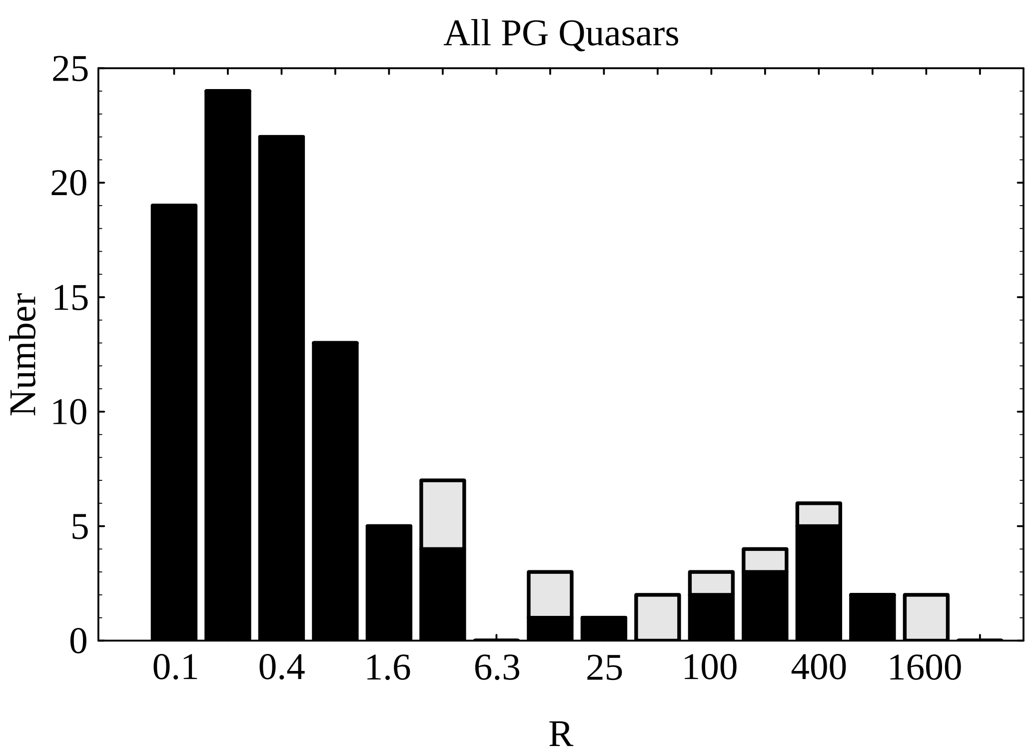
All PG Quasars
Number
R
0.1
0.4
1.6
6.3
25
100
400
1600
0
5
10
15
20
25